Lawrence Berkeley National Laboratory
Chemical Sciences

Title
Electron interaction with dimethyl disulfide in the low- and intermediate-energy range

Permalink

Journal

ISSN

Authors
da Silva, LA
da Mata, VAS
de Souza, GLC
et al.

Publication Date

DOI

Peer reviewed

Electron interaction with dimethyl disulfide in the low- and intermediate-energy range

L. A. da Silva,[1, *] V. A. S. da Mata,[2, *] G. L. C. de Souza,[2] I. Iga,[1] L. E. Machado,[3] R. R. Lucchese,[4] M.-T. Lee,[1] and M. G. P. Homem[1]

[1]*Departamento de Química, Universidade Federal de São Carlos,*
13565-905 São Carlos, São Paulo, Brazil

[2]*Departamento de Química, Universidade Federal do Mato Grosso,*
78060-900 Cuiabá, Mato Grosso, Brazil

[3]*Departamento de Física, Universidade Federal de São Carlos,*
13565-905 São Carlos, São Paulo, Brazil

[4]*Department of Chemistry, Texas A&M University,*
College Station, Texas 77842-3012, USA

(Dated: August 10, 2016)

Abstract

We report a joint theoretical-experimental investigation on elastic electron scattering by dimethyl disulfide (DMDS) in the low- and intermediate-energy regions. Experimental angular distributions of the elastically scattered electrons were measured in the 10–800 eV and 5°–130° range using a crossed electron beam-molecular beam geometry. The absolute values of the differential cross sections (DCS) were obtained using the relative-flow technique. Also, integral (ICS) and momentum-transfer (MTCS) cross sections were derived from the experimental DCS via a numerical integration procedure. Theoretically, DCS, ICS, MTCS, grand-total (TCS) and total absorption (TACS) cross sections are reported in the 1–500 eV range. In our calculations, a complex optical potential was used to represent the collision dynamics and a single-center expansion method combined with the Padé approximation was used to solve the scattering equations. Our experimental data are in good agreement with the present calculated data. Comparisons with other theoretical results are also made.

PACS numbers: 34.80.Bm

---

* L. da Silva and V. da Mata contributed equally to this work.

I. INTRODUCTION

Among numerous small sulfur-containing compounds, dimethyl disulfide (DMDS) is particularly interesting due to the presence of a S-S (disulfide) bond. This bond is similar to the S-S bridges present in several proteins which are fundamental for stabilizing the secondary structures [1, 2] of such macromolecules. Therefore, DMDS is an important prototype system for biophysics and biochemistry and has attracted attention in the scientific community during the past years.

Since the disulfide bridge cleavage in proteins can be induced by the reaction with electrons, studies involving electron interaction with DMDS are certainly very relevant and have been a subject of many recent investigations. For instance, electron-transmission (ET) spectrum of DMDS was reported by Dezarnaud-Dandine *et al.* [3]. A shape resonance of σ_{S-S} nature was observed in that study. More recently, dissociative-attachment spectrum of DMDS was reported by Matias *et al.* [4]. Resonancelike features located at about 1 eV were also seen in their anion efficiency curves of the SCH_2^-, SCH_3^- and $S_2CH_3^-$ fragments. On the theoretical side, two investigations on electron scattering by DMDS appeared recently in the literature. In 2014, Santos *et al.* [5] reported a study of electron interaction with DMDS at incident energies up to 12 eV using the Schwinger multichannel method (SMC). Shape resonances of σ_{S-S} and σ_{S-C} natures were revealed in their ICS calculated using different approaches for the interaction potentials. More recently, Kaur *et al.* [6] reported ICS, TCS, and total ionization cross sections (TICS) for electron scattering by DMDS in the incident energy range from few eV to 5 keV. A multi-scattering center spherical complex optical potential (MSCOP) formalism was employed in their calculations. Nevertheless, we observed that there is a lack of any kind of experimental cross sections as well as theoretical DCS for electron scattering by this target.

Recently, our group reported a joint experimental-theoretical investigation on electron scattering by dimethyl sulfide (DMS) [7]. In that study, experimental DCS, ICS and MTCS were measured in the 30–800 eV energy range whereas theoretical DCS, ICS, MTCS, TCS, and TACS were calculated in the 1–500 eV range. The calculations were carried out using a combination of the molecular complex optical potential (MCOP) model with the Padé approximation. In the overlapped energy range, a good agreement between our measured and theoretical data was verified. Moreover, the calculated ICS and MTCS for DMS showed

a broad peak centered at about 6 eV which is a superposition of several shape resonances of σ_{S-C} nature.

In this work, we extend such joint investigation to electron interaction with DMDS. Basically, the same experimental and theoretical techniques used for DMS [7] are employed in the present study, except the measurement of the DCS of DMDS was extended at energies down to 10 eV.

The organization of this work is as follows: In Sec. II, we present briefly the experimental procedure. In Sec. III, the used theory and details of the calculations are presented. In Sec. IV, we present our calculated and measured data. Comparisons with the existing theoretical data [5, 6] in the overlapping energies are also shown. Finally, some conclusion remarks are presented.

II. EXPERIMENTAL

The experimental setup used in the present measurements is the same as described in our previous works [7–10]. The elastically scattered electrons by DMDS were measured using a crossed electron beam-molecular beam geometry and were energy-filtered by a retarding-field analyzer with a resolution of about 1.5 eV. This analyzer is able to discriminate the electronic excitation inelastic electrons, but not those from vibrational excitations. Therefore, our reported results are indeed vibrationally-summed cross sections.

The liquid phase DMDS was purchased from Sigma-Aldrich with a purity better than 99%. Gaseous DMDS was obtained from the saturated vapor above a liquid sample in a small vial attached to the gas handling system. Details of our sample handling system were also described previously [11]. Several cycles of freeze-pump-thaw degassing were performed in order to eliminate the atmospheric air and other volatile contaminants. The purity of the gaseous DMDS was checked during the measurements using a quadrupole mass analyzer attached to the experimental chamber.

The angular distributions of scattered electrons were converted to absolute DCS using the relative-flow technique (RFT) [12]. Argon and nitrogen were used as secondary standards. Therefore,

$$\left(\frac{d\sigma}{d\Omega} \right)_x = \left(\frac{d\sigma}{d\Omega} \right)_{std} \frac{I_x}{I_{std}} \frac{n_{std}}{n_x} \left(\frac{M_{std}}{M_x} \right)^{\frac{1}{2}}, \tag{1}$$

3

where x refers to the target under study, std is the secondary stardard, I is the scattered intensity, n is the relative flow rate and M is the molecular weight. In general, for backing pressures (P) up to around 3–4 Torr, the flow rate can be written as $n = k_1 P + k_2 P^2$ [11]. However, due to the very low volatility of DMDS, the normalization procedure in this work was performed in a low pressure regime ($P < 0.3$ Torr). Thus, the second order contributions were neglected and the application of the RFT reduces to:

$$\left(\frac{d\sigma}{d\Omega}\right)_x = \left(\frac{d\sigma}{d\Omega}\right)_{std} \frac{I_x}{I_{std}} \frac{P_{std}}{P_x}. \tag{2}$$

Also, the pressures of DMDS and the secondary standard were chosen to ensure the condition of equal mean-free-path [12], that is:

$$\frac{P_x}{P_{std}} = \frac{\delta_{std}^2}{\delta_x^2}, \tag{3}$$

where δ is the atomic or molecular diameter. In this work, $\delta_{Ar} = 2.94$ Å [13], $\delta_{N_2} = 3.14$ Å [13], and $\delta_{DMDS} = 4.41$ Å were used. The latter was calculated from the Van der Waals gas model using the critical constants reported in the literature [14].

At energies up to 30 eV, the experimental DCS of N_2 reported by Shyn and Carignan [15] were used to normalize our data. At higher energies, Ar was used as secondary standard. Specifically, the absolute DCS of Dubois and Rudd [16] at 50 and 800 eV and the DCS reported by Jansen [17] in the 100–500 eV range were used. The estimated overall uncertainties in the present DCS are 16.5% at 800 eV and at 30 eV and below, 21% at 50 eV, and 11% at other energies.

The experimental ICS and MTCS in the 20–800 eV were obtained by a numerical integration over the DCS. For that, DCS at angular regions not covered in the experiments were estimated by extrapolation following the trend of the MCOP calculations. At 150 eV and above and at angles larger than 130°, the extrapolated DCS were obtained following the trend of the IAM. The overall uncertainties were estimated to be 30% at 20, 30 and 50 eV, and 25% at other energies. This procedure was not applied to obtain the ICS and MTCS at 10 eV because the DCS at this energy were measured from 25° and therefore an accurate extrapolation towards small angles would be difficult.

III. THEORY AND NUMERICAL PROCEDURE

The theory used here is essentially the same as in some of our previous works [7, 9, 10, 18]. Briefly, the dynamics of electron-target interaction is represented by a complex optical potential (U_{opt}) composed of static (U_{st}), exchange (U_{ex}), correlation-polarization (U_{cp}), and absorption (U_{ab}) contributions. Therefore, the many-body nature of the electron-molecule interaction was reduced to an one-particle scattering problem. In the present work, U_{st} and U_{ex} were derived exactly from a near-Hartree-Fock self-consistent-field (HF-SCF) target wave function, whereas U_{cp} was obtained in the framework of the free-electron-gas model, derived from a parameter-free local density [19]. The absorption potential U_{ab} is the scaled quasi-free scattering model (SQFSM) absorption potential of Lee *et al.* [20] which is an improvement of the version 3 of the model absorption potential originally proposed by Staszewska *et al.* [21]. Further, the scattering equation is solved iteratively using the [N/N] Padé approximation [22] according to the technique described in our previous works [7, 9, 10, 18].

The HF-SCF wave function of DMDS was obtained using the triple-zeta valence (TZV-3d) basis set of the GAMESS package [23]. The point group C_2 was used in our calculations. At the experimental ground-state molecular geometry [24], this basis provided a total energy of -874.3336 hartrees. The calculated electric dipole moment was 2.20 D, about 20% over-estimated with respect to the experimental value of 1.85 D [13]. Moreover, the asymptotic form of U_{cp} was generated using the dipole polarizabilities $\alpha_{xx} = 57.76$ a.u., $\alpha_{yy} = 83.39$ a.u., and $\alpha_{zz} = 60.55$ a.u., taken from the literature [24]. They were calculated at the HF-SCF level using the aug-cc-pTZV basis set. In our calculation, the wave functions and interaction potentials, as well as the related matrices, were all single-center expanded about the center-of-mass of the molecule in terms of the symmetry-adapted functions [25]. The truncation parameters used in these expansions were $l_c = 30$ for the angular momenta and $h_c = 30$ for their projections for all bound orbitals and the interaction potentials. These cut-off parameters were also used for the continuum orbitals and T-matrix elements at 200 eV and above. At lower energies, $l_c = 20$ and $h_c = 20$ were used. The calculated cross sections were converged up to 10 iterations. Also, due to the polar nature of the DMDS, a Born-closure formula was used in order to recover the effects of high partial-wave contributions to the scattering amplitudes. The procedure was the same as used in some of our

previous studies [26–28].

For the sake of completeness, we also performed calculations of DCS, ICS, MTCS for elastic e^-–DMDS scattering in the IAM framework. Using the IAM, the DCS is written as:

$$\frac{d\sigma}{d\Omega} = \sum_{i,j}^{N_a} f_i(\theta, k) f_j^*(\theta, k) \frac{sin(sr_{ij})}{sr_{ij}}, \tag{4}$$

where $f_i(\theta, k)$ is the complex scattering amplitude due to the i-th atom in a molecule, r_{ij} is the internuclear distance between atoms i and j, and $s = 2ksin\left(\frac{\theta}{2}\right)$ is the magnitude of the transferred momentum during the collision. The sum extends over the N_a atoms of the molecule. The atomic scattering amplitudes were obtained by solving the partial-wave radial Schrödinger equation at the static-exchange-polarization-absorption level of approximation:

$$\left(\frac{d^2}{dr^2} - \frac{l(l+1)}{r^2} - U_{opt} + k^2\right) u_l(r) = 0. \tag{5}$$

The static atomic potentials were given by Salvat *et al.* [29] and a model potential proposed by Furness and McCarthy [30] was used to account for the exchange contributions. The model polarization potential of Padial and Norcross [19] and the SQFSM absorption potential of Lee *et al.* [20] were also accounted for. The atomic polarizabilities, as well as the internuclear distances used in the calculations were taken from the literature [13, 24].

IV. RESULTS AND DISCUSSION

Our experimental DCS, ICS, and MTCS for elastic electron scattering by DMDS are listed in Table 1. A comparison of these experimental DCS with our theoretical results, calculated at both the MCOP and the IAM levels of approximation, are shown in Figs. 1–4. There is a general good agreement between our experimental DCS and the theoretical data calculated using the MCOP and Padé approximation. Particularly, the oscillations seen in the experimental DCS are well reproduced by our theory. On the other hand, the MCOP calculations underestimate the DCS at 500 eV for scattering angles larger than 110°. This behavior was already observed for other targets [7, 9] and was attributed to the poor convergence in the single-center expansions of the nuclear part of the interaction potential for atoms a few angstrons away from the origin. The effect of such lack of convergence manifests more significantly for high-energy electrons due to their deeper penetration power into the target. On the other hand, the DCS calculated using the IAM generally overestimate

the experimental data, mainly for incident energies up to 200 eV. However, the agreement between the IAM and the experimental data improves with increasing energies. In particular at 500 eV and large scattering angles, the IAM DCS are even in better agreement with the measured data than those calculated using the MCOP. This is due to the multicenter nature of the interaction potential used in the IAM calculations [31].

At energies below 10 eV, there is neither experimental nor other theoretical DCS to compare with our calculations. For the sake of completeness, some MCOP DCS in the 1–8 eV energy range are shown in a figure included in the Supplemental Material [32].

In Fig. 5, we compare our theoretical ICS and MTCS calculated using the MCOP with the present experimental data. The SMC ICS of Santos *et al.* [5] up to 12 eV calculated at their second version of the static-exchange-polarization (SEP2) level of approximation, the MSCOP ICS of Kaur *et al.* [6] in the 30–500 eV range, and the present results of ICS and MTCS calculated using the IAM additivity rule (AR) approach are also shown. Moreover, the ET spectrum of Dezarnaud-Dandine *et al.* [3] scaled by a factor of hundred is included in this figure as well. In general, there is a very good agreement between our MCOP ICS and MTCS and our measured data in the 30–500 eV range. The present IAM-AR calculations overestimate the MCOP ICS at energies below 50 eV and systematically overestimate the MCOP MTCS. On the other hand, the calculated ICS of Kaur *et al.* strongly underestimate both the MCOP and experimental ICS. At low incident energies, there is a fair agreement between our MCOP ICS and those of Santos *et al.*.

Moreover, there are two bumps located at about 3 and 6 eV, respectively, in both our MCOP ICS and MTCS. In our previous study for DMS [7], a broad enhancement located at about 6 eV was also observed, and was identified as a composition of several shape resonances of σ_{S-C} nature. However, no evidence of resonance was observed at around 3 eV in that study. Thus, the bump at about 3 eV in our MCOP calculation is attributed to the occurrence of a shape resonance of σ_{S-S} nature in the A_1 scattering channel. In fact, such resonances were also seen in the ET spectrum of Dezarnaud-Dandine *et al.* with maxima located at about 1.5 eV (σ_{S-S}) and 3.5 eV (σ_{S-C}) and in the SMC-SEP2 calculations of Santos *et al.* located at about 0.9 eV (σ_{S-S}) and 3.2 eV (σ_{S-C}). The shifts of our calculated resonance positions to higher energies may be due to the different approach used to represent the polarization effects.

In Figs. 6(a) and 6(b), we present our MCOP TCS and TACS, respectively, for electron

scattering by DMDS in the 1–500 eV energy range. Present IAM-AR TCS and theoretical TICS, calculated using the Binary-Encounter-Bethe (BEB) approximation [33], as well as the calculated MSCOP TCS and TICS of Kaur *at al.* are also shown for comparison. Unfortunately, there are no experimental data of TCS and TICS for this target in the literature. As seen in Fig. 6(a), IAM-AR calculations overestimate the MCOP TCS at energies below 100 eV. In contrast, the calculated TCS of Kaur *at al.* systematically underestimate the MCOP TCS. Such behaviors are similar to those shown for ICS in Fig. 5(a). Also, in Fig. 6(b), our calculated TACS lie systematically above the BEB TICS. This behavior is expected, since TACS account for both excitation and ionization processes, whereas only ionization processes are accounted for in TICS. On the other hand, the TICS calculated by Kaur *et al.* significantly overestimate our TACS at energies below 200 eV.

In summary, this study reports a joint theoretical-experimental investigation on electron collision with DMDS in a wide energy range. More precisely, absolute DCS, ICS, and MTCS for elastic e^-–DMDS scattering were measured in the 10–800 eV range. Such measurements were mainly motivated by the lack of experimental cross sections for this target in the literature. The reliability of the present experimental data is supported by our theoretical investigation using a combination of MCOP and Padé approximation, and also by the present IAM calculations at the higher-end of energies. Moreover, a shape resonance of σ_{S-S} nature located at about 3 eV is identified in the A_1 symmetry. This resonance was also observed in the ET spectrum [3] and SMC-SEP2 ICS of Santos *et al.* [5], although both shifted to lower incident energies. The polarization potential used in the present work may be the origin of the discrepancy.

ACKNOWLEDGMENTS

[1] G. E. Schulz and R. H. Schirmer, *Principles of Protein Structure* (Springer-Verlag, New York, 1979).

[2] S. D. Dai, C. Schwendtmayer, P. Schurmann, S. Ramaswamy, and H. Eklund. Redox Signaling in Chloroplasts: Cleavage of Disulfides by an Iron-Sulfur Cluster. Science **287**, 655 (2000).

[3] C. Dezarnaud-Dandine, F. Bournel, M. Tronc, D. Jones, and A. Modelli. σ^* resonances in electron transmission (ETS) and x-ray absorption (XAS) spectroscopies of dimethyl(poly)sulphides $(CH_3)_2S_x(x = 1, 2, 3)$. J. Phys. B **31**, L497 (1998).

[4] C. Matias, A. Mauracher, P. Scheier, P. Limão-Vieira, and S. Denifl. Low-energy electron interactions with dimethyl disulphide. Chemical Physics Letters **605–606**, 71 (2014).

[5] J. S. dos Santos, F. Kossoski, and M. T. do N. Varella. Interaction of low-energy electrons with dimethyl sulfide and dimethyl disulfide Phys. Rev. A **90**, 052713 (2014).

[6] J. Kaur, S. Singh, and Bobby Antony. Electron scattering studies of DMS, DMDS and DMSO homologous series. Molecular Physics, 1 (2015).

[7] M. G. P. Homem, I. Iga, J. R. Ferraz, A. S. dos Santos, L. E. Machado, G. L. C. de Souza, L. M. Brescansin, R. R. Lucchese, and M.-T. Lee. Theoretical and experimental investigation of electron collisions with dimethyl sulfide. Phys. Rev. A **91**, 012713 (2015).

[8] M. G. P. Homem, R. T. Sugohara, I. P. Sanches, M. T. Lee, and I. Iga. Cross sections for elastic electron collisions with tetrahydrofuran. Phys. Rev. A **80**, 032705 (2009).

[9] M. G. P. Homem, I. Iga, L. A. da Silva, J. R. Ferraz, L. E. Machado, G. L. C. de Souza, V. A. S. da Mata, L. M. Brescansin, R. R. Lucchese, and M.-T. Lee.Theoretical and experimental investigation of electron collisions with acetone. Phys. Rev. A **92**, 032711 (2015).

[10] G. L. C. de Souza, L. A. da Silva, W. J. C. Souza, R. T. Sugohara, I. Iga, A. S. Santos, L. E. Machado, M. G. P. Homem, L. M. Brescansin, R. R. Lucchese, and M. T. Lee. Electron collisions with small esters: A joint experimental-theoretical investigation. Physical Review A **93**, 032711 (2016).

[11] M. G. P. Homem, I. Iga, R. T. Sugohara, I. P. Sanches, and M. T. Lee. Role of adsorption effects on absolute electron-molecule cross-section calibration using the relative flow technique. Rev. Sci. Instrum. **82**, 013109 (2011).

[12] S. K. Srivastava, A. Chutjian and S. Trajmar. Absolute elastic differential electron scattering

cross sections in the intermediate energy region.I. H_2. J. Chem. Phys. **63**, 2659 (1975).

[13] Handbook of Chemistry and Physics, 73rd ed., edited by David R. Lide (CRC Press, Boca Raton, 1992).

[14] D. M. VonNiederhausern, G. M. Wilson, and N. F. Giles. Critical Point and Vapor Pressure Measurements for 17 Compounds by a Low Residence Time Flow Method. J. Chem. Eng. Data **51**, 1990 (2006).

[15] T. W. Shyn and G. R. Carignan. Angular distribution of electrons elastically scattered from gases: 1.5–400 eV on N_2. II. Phys. Rev. A **22**, 923 (1980).

[16] R. D. DuBois and M. E. Rudd. Differential cross sections for elastic scattering of electrons from argon, neon, nitrogen and carbon monoxide. J. Phys. B **9**, 2657 (1976).

[17] R. H. J. Jansen, F. J. de Heer, H. J. Luyken, B. van Wingerden, and H. J. Blaauw. Absolute differential cross sections for elastic scattering of electrons by helium, neon, argon and molecular nitrogen. J. Phys. B **9**, 185 (1976).

[18] P. Rawat, M. G. P. Homem, R. T. Sugohara, I. P. Sanches, I. Iga, G. L. C. de Souza, A. S. dos Santos, R. R. Lucchese, L. E. Machado, L. M. Brescansin, and M.-T. Lee. Cross sections for electron scattering by ethane in the low- and intermediate-energy ranges. J. Phys. B **43**, 225202 (2010).

[19] N. T. Padial and D. W. Norcross. Parameter-free model of the correlation-polarization potential for electron-molecule collisions. Phys. Rev. A **29**, 1742 (1984).

[20] M.-T. Lee, I. Iga, L. E. Machado, L. M. Brescansin, E. A. y Castro, I. P. Sanches, and G. L. C. de Souza. Improvement on the complex optical potential for electron collisions with atoms and molecules. J. Electron Spectrosc. Relat. Phenom. **155**, 14 (2007).

[21] G. Staszewska, D. W. Schwenke, and D. G. Truhlar. Investigation of the shape of the imaginary part of the optical–model potential for electron scattering by rare gases. Phys. Rev. A **29**, 3078 (1984).

[22] F. A. Gianturco, R. R. Lucchese, and N. Sanna. On the scattering of low-energy electrons by sulphur hexafluoride. J. Chem. Phys. **102**, 5743 (1995).

[23] M. W. Schmidt, K. K. Baldridge, J. A. Boatz, S. T. Elbert, M. S. Gordon, J. H. Jensen, S. Koseki, N. Matsunaga, K. A. Nguyen, S. Su, T. L. Windus, M. Dupuis, and J. A. Montgomery, J. Comput. Chem. **14**, 1347 (1993).

[24] http://cccbdb.nist.gov

[25] P. G. Burke, N. Chandra, and F. A. Gianturco. Electron-molecule interactions. IV. Scattering by polyatomic molecules. J. Phys. B **5**, 2212 (1972).

[26] L. M. Brescansin, L. E. Machado, M.-T. Lee, H. Cho and Y. S. Park. Absorption effects in intermediate-energy electron scattering by hydrogen sulphide. J. Phys. B **41**, 185201 (2008).

[27] M.T. Lee, G. L. C. de Souza, L. E. Machado, L. M. Brescansin, A. S. dos Santos, R. R. Lucchese, R. T. Sugohara, M. G. P. Homem, I. P. Sanches, and I. Iga. Electron scattering by methanol and ethanol: A joint theoretical-experimental investigation. J. Chem. Phys. **136**, 114311 (2012).

[28] L. E. Machado, L. M. Brescansin, I. Iga and M.-T. Lee. Elastic and rotational excitation cross-sections for electron-water collisions in the low- and intermediate-energy ranges. Eur. Phys. J. D **33**, 193 (2005).

[29] F. Salvat, J. D. Martinez, R. Moyol, and J. Parellada. Analytical Dirac-Hartree-Fock-Slater screening function for atoms (Z=1–92). Phys. Rev. A **36**, 467 (1987).

[30] J. B. Furness and I. E. McCarthy. Semiphenomenological optical model for electron scattering on atoms. J. Phys. B **6**, 2280 (1973).

[31] M.-T. Lee and L. C. G. Freitas. Incoherent renormalised multicentre potential model for electron-linear-molecule scattering: elastic and vibrational transition cross sections for $e^- - N_2$ and $e^- - CO$. J. Phys. B **13**, 233 (1983).

[32] See Supplemental Material at [URL will be inserted by publisher] for the MCOP DCS in the 1–8 eV range.

[33] Y.-K. Kim and M. E. Rudd. Binary-encounter-dipole model for electron-impact ionization. Phys. Rev. A **50**, 3954 (1994).
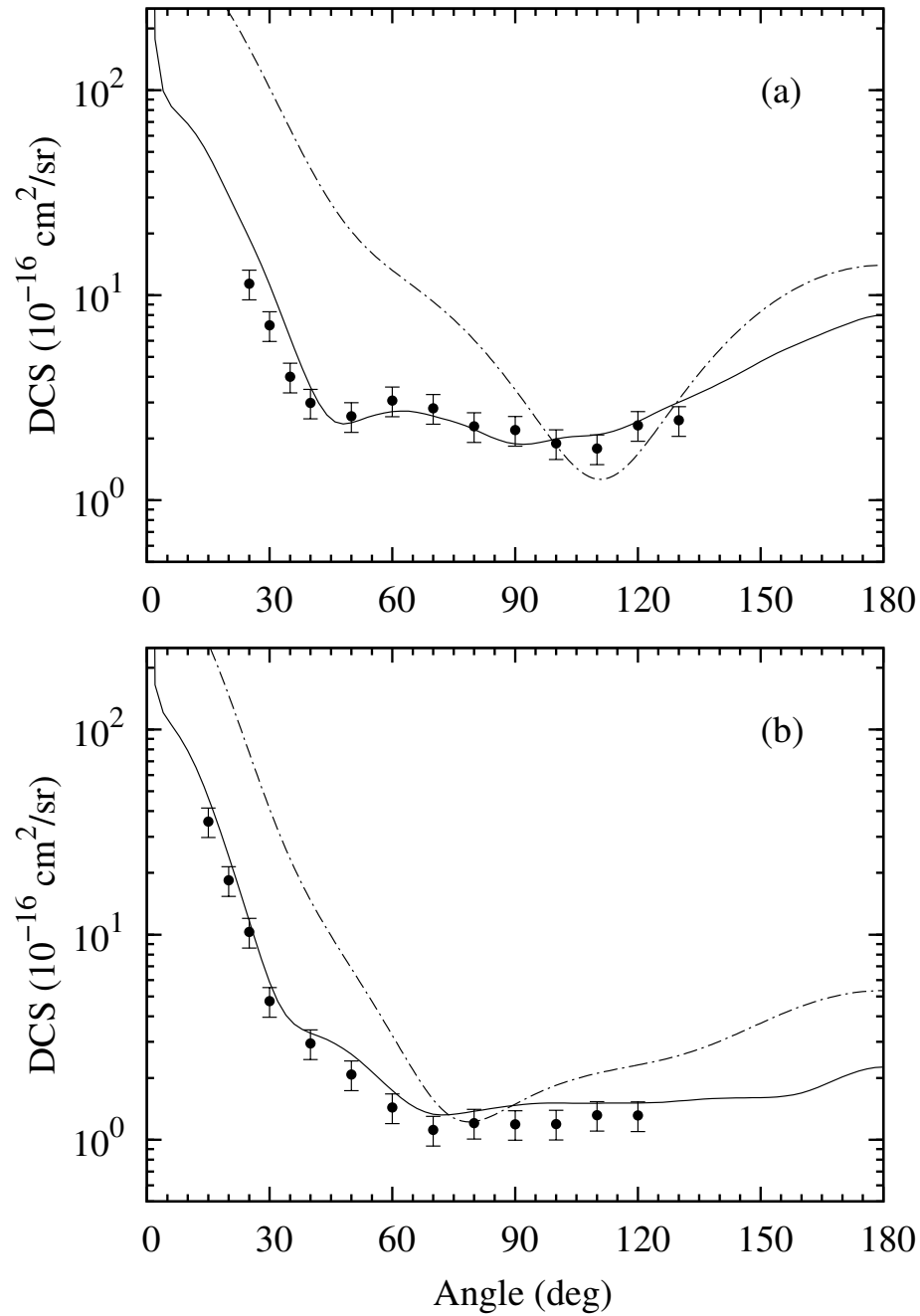
FIG. 1. DCS for elastic e^-–dimethyl disulfide scattering at (a) 10 eV and (b) 20 eV. Full curve, present MCOP results; dash-dotted curve, present IAM results; full circles, present experimental results.
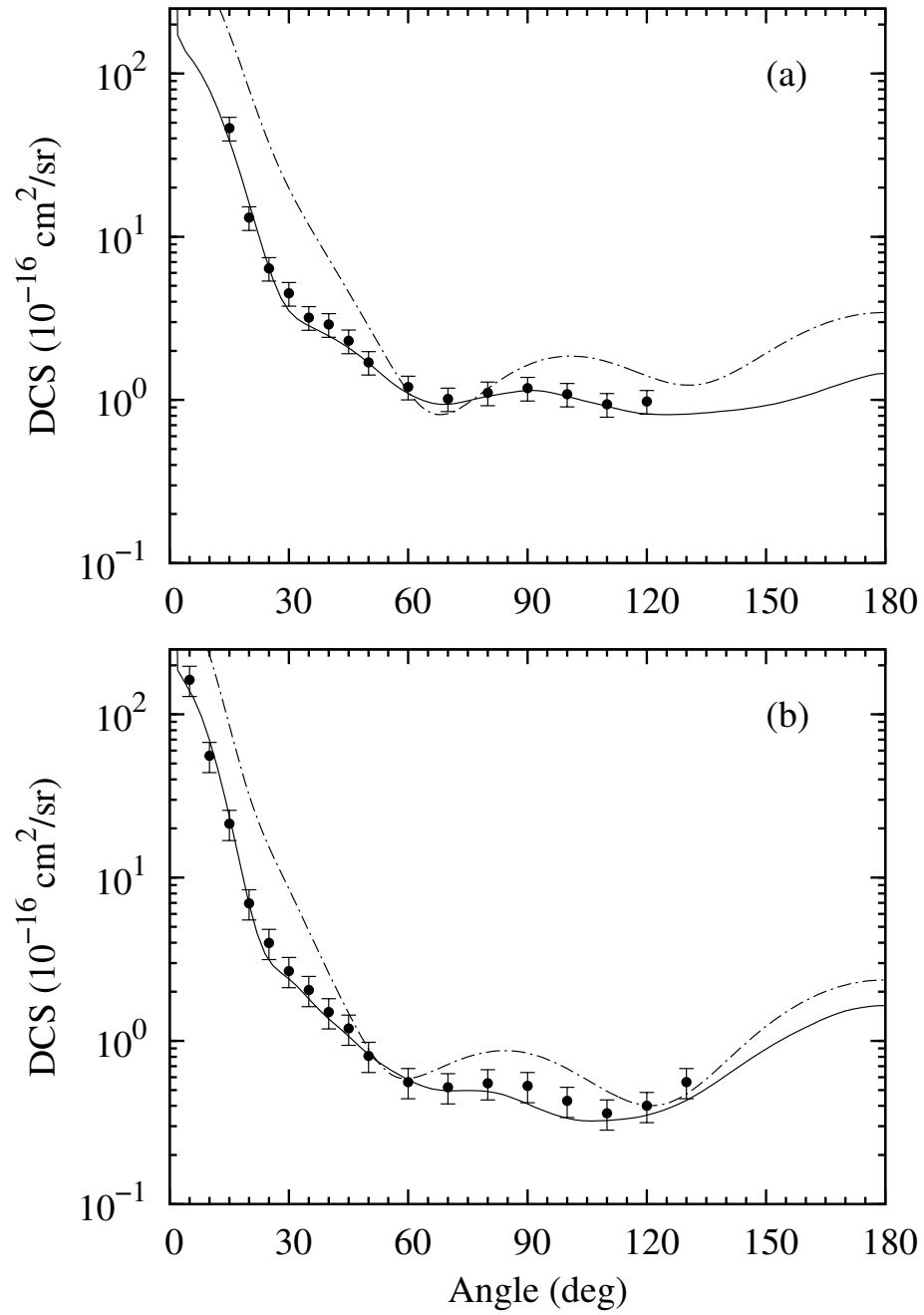
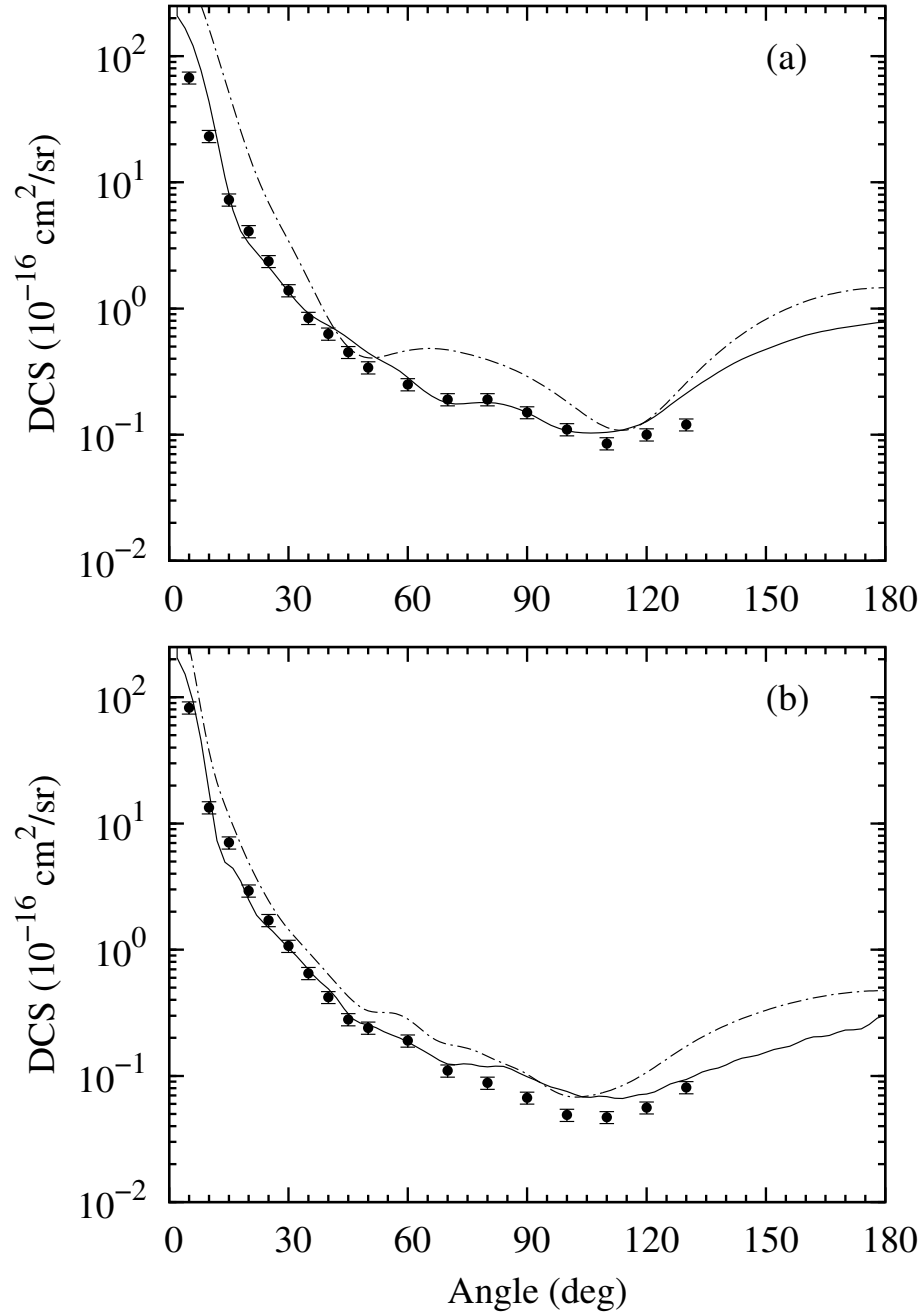FIG. 2. Same as in Fig. 1 but at (a) 30 eV and (b) 50 eV

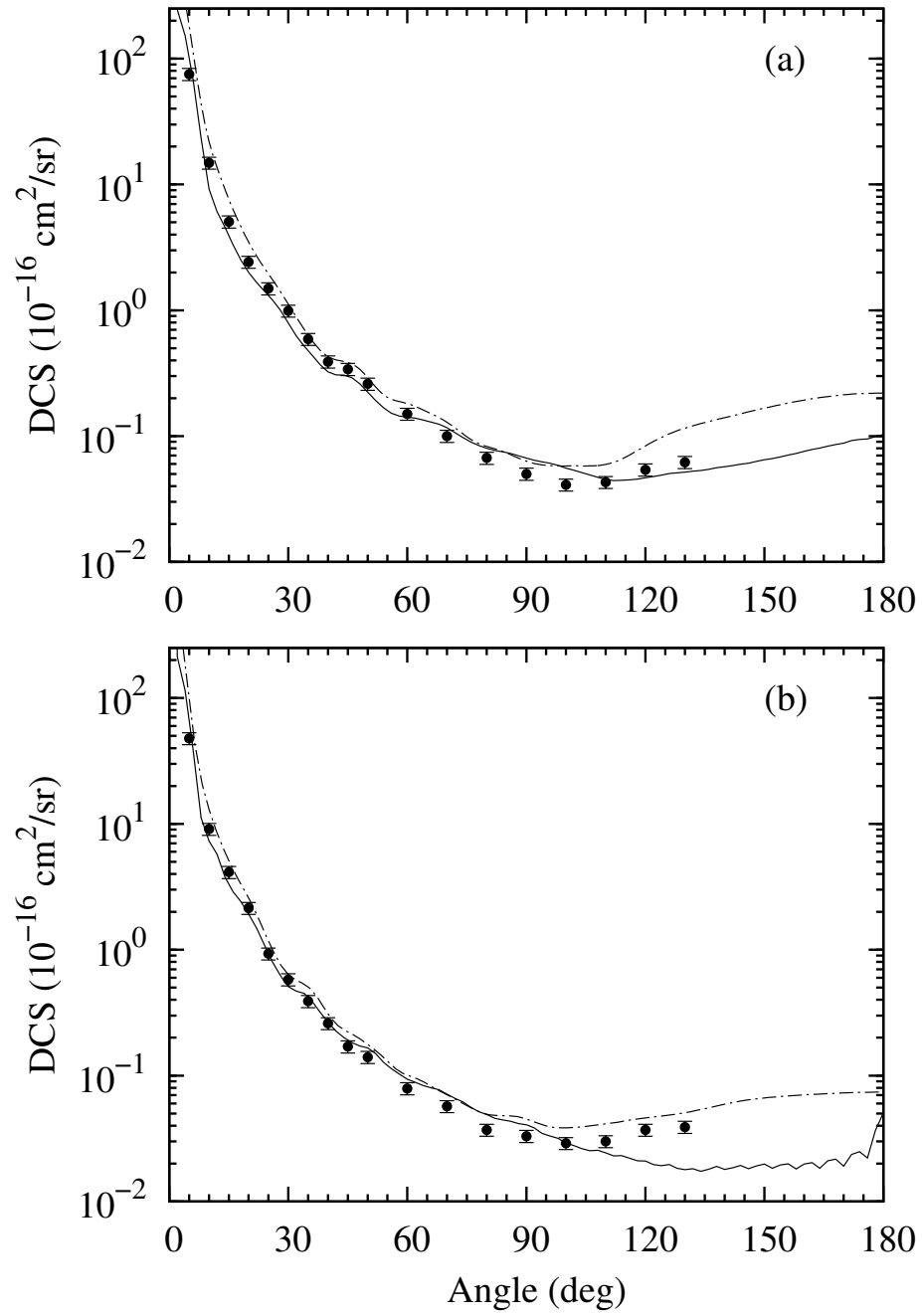FIG. 3. Same as in Fig. 1 but at (a) 100 eV and (b) 200 eV.

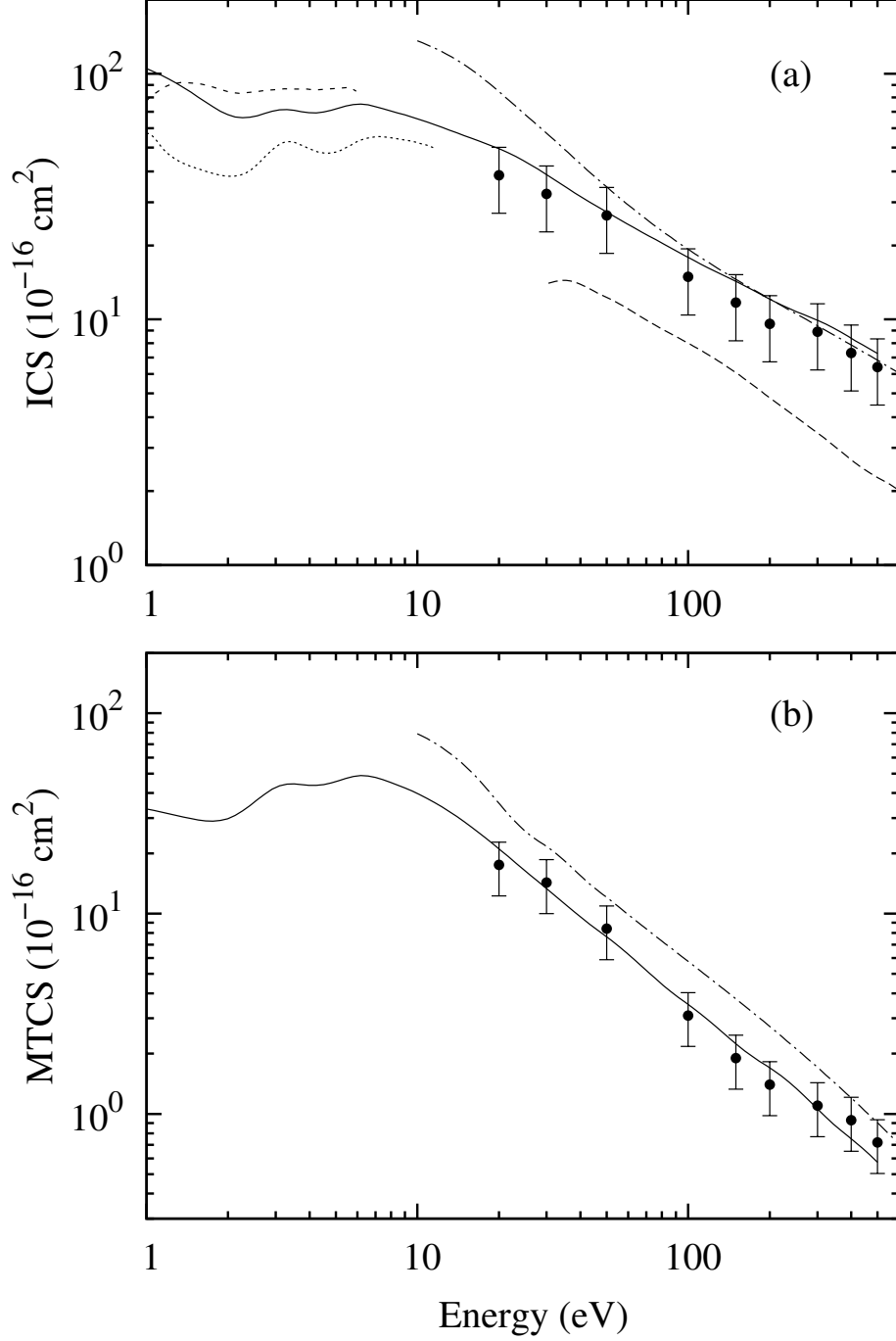FIG. 4. Same as in Fig. 1 but at (a) 300 eV and (b) 500 eV.

FIG. 5. (a) ICS and (b) MTCS for elastic e^-–dimethyl disulfide scattering. Full curve, present calculated data using the MCOP; dash-dotted curve, present calculated data using the IAM-AR; dashed curve, MSCOP ICS of Kaur *et al.* [6]; dotted curve, SMC ICS of Santos *et al.* [5]; short-dashed curve, ET spectrum of Dezarnaud-Dandine *et al.* [3] scaled by a factor of hundred; full circles, present experimental data.
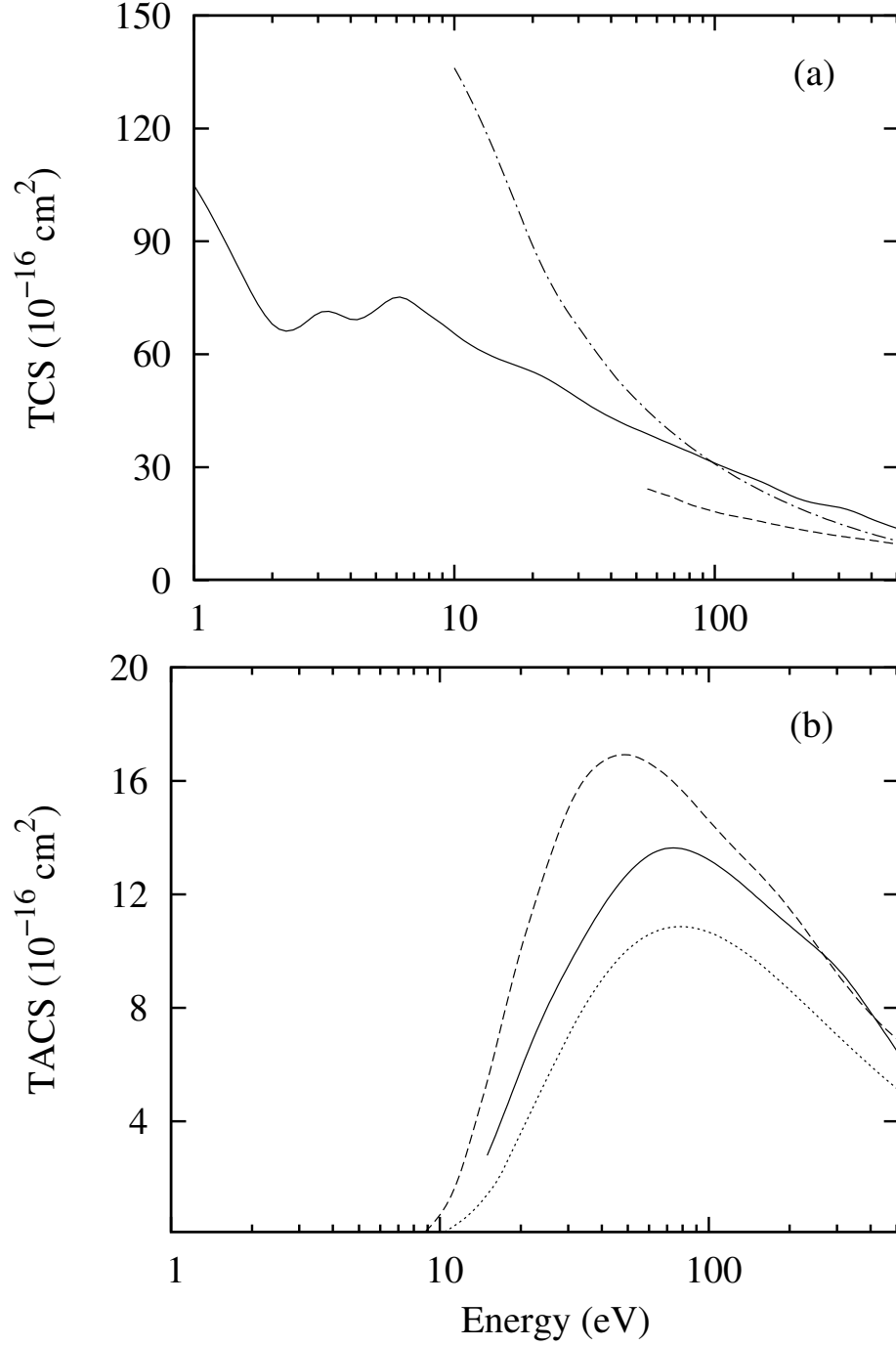
FIG. 6. (a) TCS and (b) TACS for e^-–dimethyl disulfide scattering. Full curve, present data calculated using the MCOP; dash-dotted curve, present calculated data using the IAM-AR; dashed curve, TCS and TICS of Kaur *et al.* calculated using the MSCOP [6]; dotted curve, present TICS calculated using BEB.

TABLE I. Experimental DCS (in 10^{-16} cm^2/sr), ICS and MTCS (in 10^{-16} cm^2) for elastic e$^-$-dimethyl disulfide.

Angle						E(eV)					
(deg)	10	20	30	50	100	150	200	300	400	500	800
5				162.6	67.5	105.9	82.7	75.2	36.1	47.8	25.1
10				55.7	23.2	18.9	13.4	14.8	9.9	9.1	8.5
15		35.6	30.3	21.4	7.3	7.7	7.1	5.1	4.6	4.1	3.7
20		18.4	10.8	6.9	4.1	3.5	2.9	2.4	2.7	2.1	1.3
25	11.4	10.3	6.4	3.9	2.4	1.9	1.7	1.5	1.4	0.93	0.71
30	7.1	4.7	4.5	2.7	1.4	1.0	1.1	0.99	0.73	0.58	0.42
35	4.0		3.2	2.1	0.84	0.74	0.65	0.59	0.46	0.39	0.24
40	2.9	2.9	2.9	1.5	0.63	0.53	0.42	0.39	0.37	0.26	0.17
45			2.3	0.45	0.38	0.28	0.34	0.23	0.17	0.11	
50	2.6	2.1	1.7	0.81	0.34	0.26	0.24	0.26	0.17	0.14	0.082
60	3.1	1.4	1.2	0.56	0.25	0.18	0.19	0.15	0.10	0.079	0.048
70	2.8	1.1	1.0	0.52	0.19	0.15	0.11	0.10	0.061	0.057	0.034
80	2.3	1.2	1.1	0.55	0.19	0.11	0.088	0.067	0.048	0.037	0.025
90	2.2	1.2	1.2	0.53	0.15	0.081	0.067	0.050	0.037	0.033	0.021
100	1.9	1.2	1.1	0.43	0.11	0.056	0.049	0.041	0.032	0.029	0.020
110	1.8	1.3	0.94	0.36	0.085	0.049	0.047	0.043	0.038	0.030	0.019
120	2.3	1.3	0.98	0.40	0.10	0.055	0.056	0.054	0.042	0.037	0.019
130	2.4			0.56	0.12	0.088	0.081	0.062	0.056	0.039	0.020
ICS		38.6	32.4	26.5	14.9	11.7	9.6	8.9	7.3	6.4	4.3
MTCS		17.5	14.3	8.4	3.1	1.9	1.4	1.1	0.93	0.72	0.41